Inorg. Chem. **2007**, *46*, 2604–2611

Electronic Localization versus Delocalization Determined by the Binding of the Linker in an Isomer Pair

F. Albert Cotton,*,† Chun Y. Liu,*,†,‡ Carlos A. Murillo,*,† and Qinliang Zhao†

Department of Chemistry and Laboratory for Molecular Structure and Bonding, P. O. Box 3012, Texas A&M University, College Station, Texas 77842-3012, and Department of Chemistry, Tongji University, Shanghai 200092, P. R. China

Received November 22, 2006

By using stoichiometric amounts of $(C_5H_5)_2FePF_6$, the isomeric neutral diamidate-bridged molecules, α- and β-$(DAniF)_3Mo_2(ArN(O)CC(O)NAr)Mo_2(DAniF)_3$, with Ar = *p*-$MeOC_6H_4$, have been oxidized to give the PF_6 salts of the four cations α^{1+}, α^{2+}, β^{1+}, and β^{2+}. All four structures have been accurately determined and, together with supporting evidence from near-IR, EPR, NMR and magnetic susceptibility measurements, it clearly establishes that in the mixed-valent α^{+} species the unpaired electron is localized over only one of the Mo_2 units while the α^{2+} cation behaves as a diradical having two Mo_2^{5+} units that are essentially uncoupled. However, the β^{+} species is fully delocalized, in the time scale of the experiments, with the unpaired electron being equally shared by the two Mo_2 units. It displays a HOMO−1 → SOMO transition at 4700 cm^{-1} ($\Delta\nu_{1/2}$ = 2300 cm^{-1}). Because of strong coupling, the β^{2+} species is diamagnetic.

Introduction

Mixed-valence chemistry, which deals with compounds having two or more bridged metal complex units in different formal oxidation states, has long focused on electronic interactions between adjacent, especially covalently connected, metal centers joined by a linker.[1] Much work in this area has been done on compounds that have two structurally identical metal centers united by a symmetrical organic ligand.[2] The pyrazine-bridged Ru dimer, $\{[Ru(NH_3)_5](pyz)[Ru(NH_3)_5]\}^{5+}$ (**I** in Scheme 1), also known as the Creutz−Taube ion, is the prototype.[3] Intensive studies on this and other similar compounds have aimed at answering the question of whether the unpaired electron is localized or delocalized. Conventionally, compounds are classified in the widely accepted Robin−Day categories,[4] that is, Class I (no interaction, localized valency), Class II (weak to medium coupling, valence trapped), and Class III (strong interaction, delocalized). However, assignment to these classes may not be unambiguous and consistent with the results from various

Scheme 1

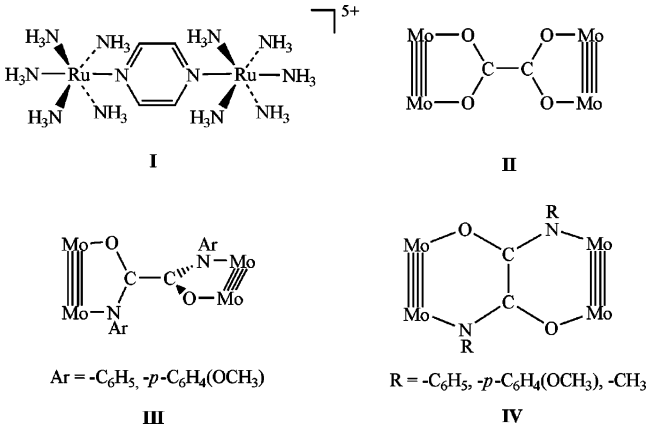

* To whom correspondence should be addressed. E-mail: cotton@tamu.edu (F.A.C.); cyliu05@gmail.com (C.Y.L.); murillo@tamu.edu (C.A.M.).
† Texas A&M University.
‡ Tongji University.

(1) (a) Prassides, K. Ed. *Mixed-valency Systems. Applications in Chemistry, Physics and Biology*; Kluwer Academic Publishers: Dordrecht, The Netherlands, 1991. (b) Blondin, G.; Gired, J.-J. *Chem. Rev.* **1990**, *90*, 1359 and references therein. (c) Gamelin, D. R.; Bominaar, E. L.; Kirk, M. L.; Wieghardt, K.; Solomon, E. I. *J. Am. Chem. Soc.* **1996**, *118*, 8085 and references therein. (d) Cotton, F. A.; Lin, C.; Murillo, C. A. *Acc. Chem. Res.* **2001**, *34*, 759. (e) Cotton, F. A.; Lin, C.; Murillo, C. A. *Proc. Nat. Acad. Sci. U.S.A.* **2002**, *99*, 4810. (f) Chisholm, M. H.; Macintosh, A. M. *Chem. Rev.* **2005**, *105*, 2949.

(2) (a) Creutz, C. *Prog. Inorg. Chem.* **1983**, *30*, 1. (b) Richardson, D. E.; Taube, H. *Coord. Chem. Rev.* **1984**, *60*, 107. (c) Demadis, K. D.; Hartshorn, C. M.; Meyer, T. J. *Chem. Rev.* **2001**, *101*, 2655. (d) Kaim, W.; Klein, A.; Glöckle, M. *Acc. Chem. Res.* **2000**, *33*, 755. (e) Dogan, A.; Sarkar, B.; Klein, A.; Lissner, F.; Schleid, T.; Fiedler, J.; Zalis, S.; Jain, V. K.; Kaim, W. *Inorg. Chem.* **2004**, *43*, 5973. (f) Rigaut, S.; Olivier, C.; Costuas, K.; Choua, S.; Fadhel, O.; Massue, J.; Turek, P.; Saillard, J.-Y.; Dixneuf, P. H.; Touchard, D. *J. Am. Chem. Soc.* **2006**, *128*, 5859. (g) D'Alessandro, D. M.; Dinolfo, P. H.; Davies, M. S.; Hupp, J. T.; Keene, F. R. *Inorg. Chem.* **2006**, *45*, 3261.

10.1021/ic0622252 CCC: $37.00
Published on Web 02/13/2007

experimental methods, even for the Creutz−Taube complex,[5] which is generally considered to be an example of strong coupling, though not necessarily delocalization.[6] Many other compounds studied are weakly coupled. Therefore, there is still a need to develop complex systems that exhibit consistent and comprehensive chemical and physical characteristics that place them unambiguously in one of the three classes proposed by Robin and Day.

Another important issue concerns the mechanism of electron delocalization for compounds that are unambiguously in Class III. It is generally understood that the electronic structure of the linker plays a critical role, through metal−ligand orbital interaction, in the distribution of an odd electron from end to end of the molecule. For example, theoretical work on the Creutz−Taube ion has indicated that π back-bonding interaction that occurs between filled Ru d_{xy} orbitals and the empty π^* orbitals of pyrazine has a major influence on the overall electronic configuration of the complex.[7] There is no doubt that the efficiency of such orbital overlap has an important effect on electron delocalization. Therefore, it is necessary to tune the efficiency of the orbital overlap to control a ligand-mediated electron-transfer process. This tuning can be done by varying characteristics of the linker such as conformation, conjugation, binding mode, and length, to name only a few of the main factors. A general understanding of electronic coupling interactions has provided valuable guidance for the synthesis and characterization of mixed-valence complexes[8] and the development of molecular electronic applications, for example, in molecular wires and molecular switches.[9]

In recent years, we[10] and others[11] have taken a different approach to this field by employing two or more dimetal units, typically two Mo_2^{4+} species joined by an appropriate linker. In such compounds, quadruply bonded Mo_2^{4+} units often act as redox sites. In our laboratory, the compounds that have been most studied may be generically formulated as $[Mo_2]L[Mo_2]$, where $[Mo_2]$ is an abbreviation for an Mo_2^{4+} core supported by three *N*,*N*′-di(*p*-anisyl)formamidinate (DAniF) anions, that is $[Mo_2(DAniF)_3]^+$, and L is a tetradentate ligand with two bidentate groups capable of binding the $[Mo_2]$ units, for example, a dicarboxylate species, $^-O_2C-X-CO_2^-$. To some extent, a quadruply bonded Mo_2^{4+} unit behaves like a single metal ion and the tetranuclear complexes $[Mo_2]L[Mo_2]$ have a basic kinship with the binuclear Creutz−Taube ion. For instance, the $[Mo_2]$ unit is an electrochemically addressable redox center in which one-electron oxidation from Mo_2^{4+} to Mo_2^{5+} occurs reversibly, and the "dimer of dimers" displays two successive redox couples with varying potential separations ($\Delta E_{1/2}$) that depend on the efficiency by which the linker allows electronic communication between the metal centers. On the other hand, a dimetal unit such as $[Mo_2]$ differs from a mononuclear ion in coordination binding mode and electronic configuration, which endow the dimolybdenum molecules with unique structural and electronic features that facilitate the study of mixed-valence chemistry. Given the equatorial binding mode for an $[Mo_2]$ unit, symmetry considerations indicate that metal-to-linker interactions may occur between the δ (metal) and π^* (ligand) orbitals.[12] A major advantage of using an $[Mo_2]$ unit in the study of mixed-valence (MV) species is that the metal−metal bond length can be precisely measured, thus affording a uniquely practical criterion for determination of the bond order or oxidation state of the dimetal center.[13] Our studies on various compounds of the type $[Mo_2]L[Mo_2]$ have shown that the nature of the linker (L) may affect the strength of the coupling interaction and the MV species may vary from being localized to being fully delocalized. For example, fully localized (Class I) mixed-valence compounds $[Mo_2]^0(OCH_3)_2M(OCH_3)_2[Mo_2]^{1+}$ (M = Zn, Co) were obtained when the tetrahedral linkers $M(OCH_3)_4^{2-}$ were used.[14] In the oxalate-linked compound $[Mo_2](O_2C-CO_2)[Mo_2]$ (**II** in Scheme 1), there are two essentially parallel dimetal units separated by a short distance, ca. 7.0 Å, which are only moderately coupled.[10] When certain large conjugated linkers are introduced, for instance, tetraazatetracene[15]and dioxolene,[16] strong metal-to-metal interaction is observed and the derived MV complexes are delocalized (Class III).

In prior work, we have reported that when a diaryloxamidate group, $[ArNC(O)C(O)NAr]^{2-}$ (Ar = phenyl or

(3) (a) Creutz, C.; Taube, H. *J. Am. Chem. Soc.* **1969**, *91*, 3988. (b) Creutz, C.; Taube, H. *J. Am. Chem. Soc.* **1973**, *95*, 1086.
(4) Robin, M. B.; Day, P. *Adv. Inorg. Chem. Radiochem.* **1967**, *10*, 357.
(5) (a) Stebler, A.; Ammeter, J. H.; Füerholz, U.; Ludi, A. *Inorg. Chem.* **1984**, *23*, 2764. (b) Bunker, B. C.; Drago, R. S.; Hendrickson, D. N.; Richman, R. M.; Kessel, S. L. *J. Am. Chem. Soc*. **1978**, *100*, 3805.
(6) In any discussion of whether a species is localized or delocalized, it is important to keep in mind the time scale of the experiments. For a note on time frames see: Lever, A. B. P. In *Comprehensive Coordination Chemistry II*; McCleverty, J. A., Meyer, T. J., Eds.; Elsevier: Amsterdam, 2004; Vol. 2, p 435.
(7) (a) Bencini, A.; Ciofini, I.; Daul, C. A.; Ferretti, A. *J. Am. Chem. Soc*. **1999**, *121*, 11418. (b) Creager, S.; Yu, C. J.; Bamdad, C.; O'Connor, S.; MacLean, T.; Lam, E.; Chong, Y.; Olsen, G. T.; Luo, J.; Gozin, M.; Kayyem, J. F. *J. Am. Chem. Soc*. **1999**, *121*, 1059.
(8) Crutchley, R. J. *Adv. Inorg. Chem.* **1994**, *41*, 273.
(9) (a) Ward, M. D. *Chem. Soc. Rev.* **1995**, *24*, 121. (b) Launay, J.-P. *Chem. Soc. Rev.* **2001**, *30*, 386. (c) Astruc, D. *Acc. Chem. Res.* **1997**, *30*, 383. (d) McCleverty, J. A.; Ward, M. D. *Acc. Chem. Res.* **1998**, *31*, 842.
(10) See for example: (a) Cotton, F. A.; Murillo, C. A.; Yu, R.; Zhao, Q. *Inorg. Chem.* **2006**, *45*, 9046. (b) Cotton, F. A.; Liu, C. Y.; Murillo, C. A.; Zhao, Q. *Inorg. Chem.* **2006**, *45*, 9493. (c) Cotton, F. A.; Liu, C. Y.; Murillo, C. A.; Zhao, Q. *Inorg. Chem.* **2006**, *45*, 9480. (d) Cotton, F. A.; Donahue, J. P.; Lin, C.; Murillo, C. A. *Inorg. Chem.* **2001**, *40*, 1234. (e) Cotton, F. A.; Donahue, J. P.; Murillo, C. A. *J. Am. Chem. Soc.* **2003**, *125*, 5436.
(11) (a) Chisholm, M. H.; Patmore, N. J. *Acc. Chem. Res.* **2007**, *39*, 19. (b) Burdzinski, G. T.; Ramnauth, R.; Chisholm, M. H.; Gustafson, T. L. *J. Am. Chem. Soc.* **2006**, *128*, 6776. (c) Chisholm, M. H.; Feil, F.; Hadad, C. M.; Patmore, N. J. *J. Am. Chem. Soc*. **2005**, *127*, 18150. (d) Barybin, M. V.; Chisholm, M. H.; Dalal, N. S.; Holovics, T. H.; Patmore, N. J.; Robinson, R. E.; Zipse, D. J. *J. Am. Chem. Soc.* **2005**, *127*, 15182. (e) Bursten, B. E.; Chisholm, M. H.; D'Acchioli, J. S. *Inorg. Chem.* **2005**, *44*, 5571. (f) Chisholm, M. H.; Pate, B. D.; Wilson, P. J.; Zaleski, J. M. *Chem. Commun*. **2002**, 1084. (g) Cayton, R. H.; Chisholm, M. H.; Huffman, J. C.; Lobkovsky, E. B. *J. Am. Chem. Soc.* **1991**, *113*, 8709.
(12) Cotton, F. A.; Donahue, J. P.; Murillo, C. A.; Pérez, L. M. *J. Am. Chem. Soc.* **2003**, *125*, 5486.
(13) (a) Cotton, F. A.; Hillard, E. A.; Murillo, C. A. *Inorg. Chem.* **2002**, *41*, 1639. (b) Cotton, F. A.; Daniels, L. M.; Murillo, C. A.; Wilkinson, C. C. *J. Am. Chem. Soc.* **2002**, *124*, 9249.
(14) Cotton, F. A.; Dalal, N. S.; Liu, C. Y.; Murillo, C. A.; North, J. M.; Wang, X. *J. Am. Chem. Soc.* **2003**, *125*, 1354.
(15) Cotton, F. A.; Li, Z.; Liu, C. Y.; Murillo, C. A.; Villagrán, D. *Inorg. Chem.* **2006**, *45*, 767.
(16) Cotton, F. A.; Murillo, C. A.; Villagrán, D.; Yu, R. *J. Am. Chem. Soc.* **2006**, *128*, 3281.

Scheme 2

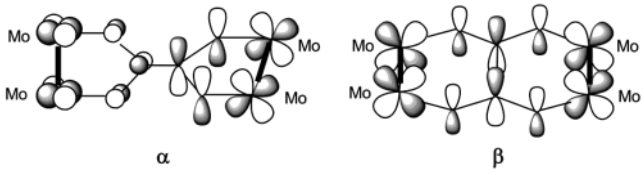

p-anisyl), serves as linker, two geometric isomers can be isolated.[17] The two isomers, designated as α (**III**) and *β* (**IV**) as shown in Scheme 1, entail different binding modes of the oxamidate ligand. The α compound has two Mo_2^{4+} units linked by the oxamidate in three-atom bridging mode, similar to the oxalate and the unsubstituted oxamidate analogues, but differing in that the two amidate groups are orthogonal. In the *β* isomer, the oxamidate linker adopts a four-atom (NCCO) bridging mode with respect to each [Mo_2] unit, thus giving a molecule with two essentially parallel Mo−Mo quadruple bonds. From their structures, it was expected that the electronic coupling effects between these two molecules should be quite different. DFT calculations[17] have shown that in the α form, the orbital interaction between two dimetal units is virtually none because of the orthogonality of the two Mo_2 units, but for the *β* isomer, delocalized molecular orbitals spread across between two Mo_2 centers with significant involvement of the ligand π^* orbitals as shown in Scheme 2. Indeed, in the primary study in which we were unable to isolate pure crystalline oxidized products,[17] we have found that while the separation of oxidation potentials ($\Delta E_{1/2}$) for the α isomer is ca.190 mV; it is ca. 530 mV for the *β* form. From these values, comproportionation constants (K_C)[18] of ca. 10^3 and 10^6 are derived for these two compounds, respectively. Furthermore, the difference between them in electronic structure is also manifested in their electronic spectra.

In the work reported here, we show that syntheses of the neutral α and *β* isomers have been improved to allow isolation of the corresponding MV species {[Mo_2](L)-[Mo_2]}$^+$, as well as the preparation of the corresponding doubly oxidized species having two linked Mo_2^{5+} units. The compounds reported here include α-[Mo_2(DAniF)$_3$]$_2$(*N*,*N*′-di-*p*-anisyloxamidate)(PF_6) (**1**), *β*-[Mo_2(DAniF)$_3$]$_2$(*N*,*N*′-di-*p*-anisyloxamidate)(PF_6) (**2**), α-[Mo_2(DAniF)$_3$]$_2$ (*N*,*N*′-di-*p*-anisyloxamidate)(PF_6)$_2$ (**3**), and *β*-[Mo_2(DAniF)$_3$]$_2$(*N*,*N*′-di-*p*-anisyloxamidate)(PF_6)$_2$ (**4**). X-ray crystallographic analyses show unambiguously that the MV species in the α form (**1**) has an unsymmetrical molecular structure with the Mo−Mo bond distances corresponding to a localized Mo_2^{4+} unit and a delocalized Mo_2^{5+} unit, whereas in the *β* form (**2**), there are two essentially identical [Mo_2] units. Consistently, these compounds also exhibit different features in the near-IR (NIR) spectra: while compound **1** has a featureless spectrum in this region, compound **2** presents an intense absorption at low energy, which might conventionally be termed a metal-to-metal intervalence charge-transfer, but which is better described as a HOMO−1 → SOMO transition in a fully delocalized molecule. The two doubly oxidized compounds in the pair also exhibit different magnetic behaviors. The α species **3** is paramagnetic because of the weakness of interactions of the two localized Mo_2^{5+} units, but the *β* form, **4**, is diamagnetic due to the pairing of the electrons in the two Mo_2^{5+} units. The two mixed-valence complexes **1** and **2** are unambiguously assigned to Class I and Class III, respectively.

Results and Discussion

Syntheses and Structural Results. In prior work, preparations for the neutral α and *β* isomers were reported. Unfortunately, the synthesis of the *β* isomer gave relatively low yields and crystals had to be manually separated.[17] In the present work, efforts have been made to improve the yield and purity of the products, particularly for the *β* isomer. The yellow α compound is now prepared by reaction of Mo_2(DAniF)$_3$(O_2CCH_3) and the neutral oxamide in tetrahydrofuran followed by addition of $NaOCH_3$ and stirring over a period of 48 h. Upon removal of the solvent and extraction of the solid with CH_2Cl_2, the product is obtained in high yield (82%) and purity. For the isolation of the pure *β* isomer, the procedure was similar to that for the α isomer but the use of a short reaction time (0.5 h) is essential. The solvent was then removed. This is followed by an extraction with CH_2Cl_2 and then addition of hot ethanol to the dichloromethane extract. To obtain a good yield and a pure product, it is important to maintain the temperature of this mixture at ∼80 °C for about half an hour. The red *β* compound precipitates from the hot ethanol/CH_2Cl_2 mixture and some byproducts, including a small amount of the soluble α isomer, are removed by filtration. It is interesting that even though both the α and *β* isomers originate from the same reactants, once formed they do not interconvert in boiling solutions of various solvents such as ethanol, THF, acetonitrile, or *o*-dichlorobenzene.

Each of these precursors (α and *β*) react with ferrocenium hexafluorophosphate, (Cp_2Fe)PF_6, to produce the oxidized compounds **1**, **2**, **3**, and **4**. The reaction stoichiometries must be strictly controlled in order to obtain the pure singly or doubly oxidized compounds. By carrying out the reactions at low temperature (−78 °C), good yields of crystalline material are generally obtained for the four compounds.

The core structure of the complex cation of **1** (α^+) is shown in Figure 1. This mono-charged dimolybdenum pair has an overall structure similar to that of the neutral precursor, with the two [Mo_2] units being orthogonal to each other. Compared to the neutral compound, the most important difference is that in **1** the two dimetal subunits are not structurally identical. In this compound one of the two Mo−Mo bonds is lengthened, relative to that in the precursor, to 2.1291(6) Å, while the other has an Mo−Mo distance (2.0920(6) Å) essentially unchanged from that in the neutral species.[17] The change in metal−metal bond distance of the first [Mo_2] unit, ca. 0.037 Å, is similar to that observed in other cases where a quadruply bonded Mo_2^{4+} unit is oxidized to an Mo_2^{5+} species, e.g., in the localized compound

(17) Cotton, F. A.; Liu, C. Y.; Murillo, C. A.; Villagrán, D.; Wang, X. *J. Am. Chem. Soc.* **2003**, *125*, 13564.
(18) Richardson, D. E.; Taube, H. *Inorg. Chem.* **1981**, *20*, 1278.

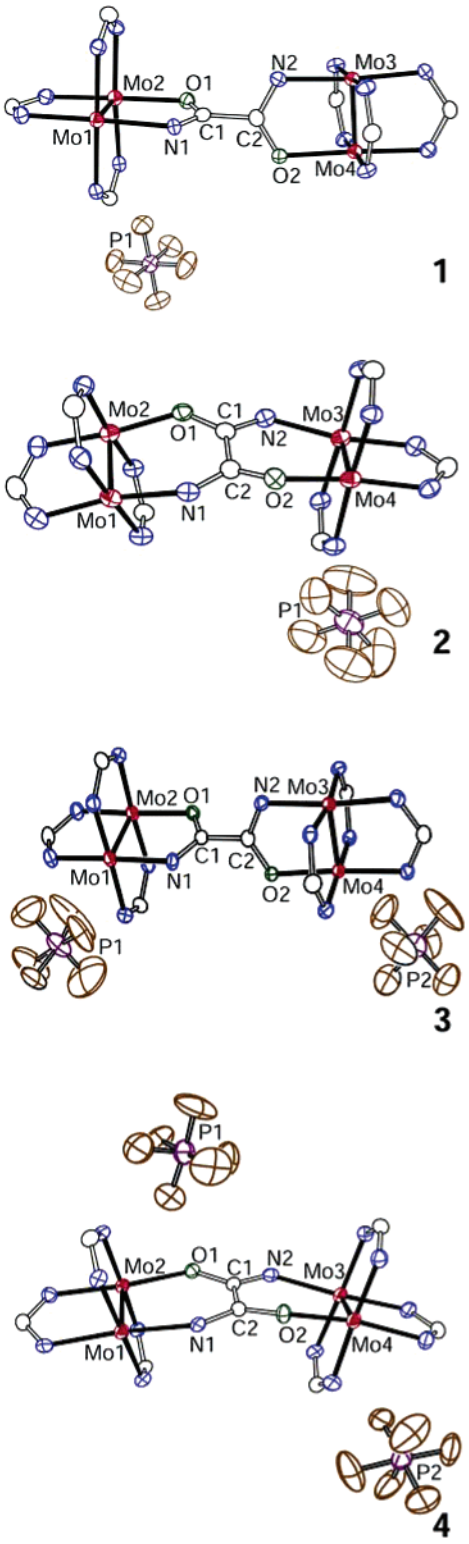

Figure 1. Core structure of **1**−**4** with ellipsoids drawn at the 40% probability level. All *p*-anisyl groups and hydrogen atoms have been omitted for clarity.

$\{[Mo_2](CH_3O)_2Zn(OCH_3)_2[Mo_2]\}^{1+}$,[14] in which the difference in bond length between the two dimolybdenum units is 0.035 Å. This indicates that only one of the Mo_2^{4+} species in the precursor has been oxidized to an Mo_2^{5+} unit. Upon oxidation of this unit, the formal bond order is lowered from 4.0 to 3.5. Consistently, there are two sets of Mo−ligand bond distances associated with the two different dimetal centers. For the oxamidate group that binds to the Mo_2^{4+} unit the Mo−N and Mo−O bond distances are 2.197(4) and 2.121(3) Å, respectively, which are about the same as those in the precursor,[17] while the corresponding bonds to the Mo_2^{5+} unit are shortened to 2.166(4) and 2.105(3) Å. The asymmetric molecular structure unambiguously indicates that compound **1** is a mixed-valence complex that belongs to the electronically localized Class I.

Compound **2** is the singly oxidized product having the β form. As shown in Figure 1, the β binding mode in the precursor is retained in the cation of **2**. The oxamidate linker binds each of the two $[Mo_2]$ units with N−C−C−O four-atom binding mode, forming two fused, six-membered, chelating rings. The two Mo_2 units are essentially parallel to each other, but the overall structure is slightly bent and twisted, as in the neutral precursor.[17] This compound has a core structure resembling the singly oxidized dimethyloxamidate-linked analogue,[19] which has been shown to be a delocalized, mixed-valence complex by various techniques, including X-ray analyses. Contrary to **1** which has two distinct Mo−Mo distances, in the isomer **2** the two crystallographically independent metal−metal bonds are equally lengthened relative to those in the parent compound. The increase in the Mo−Mo bond lengths is from 2.0944(4)[17] to 2.1116(7) and 2.1140(6) Å. The relatively small increase (ca. 0.019 Å) is attributed to the fact that formally only half an electron has been removed from each Mo_2^{4+} unit. In **2**, the metal−ligand bond distances for the two dimolybdenum units are essentially identical but shorter than those in the precursor.[17] For example, for the two Mo_2 subunits, the Mo−$N_{oxamidate}$ bonds are 2.147(4) and 2.141(4) Å and the Mo−$O_{oxamidate}$ 2.054(3) and 2.058(3) Å, while the neutral β compound has distances of 2.198(3) Å for the Mo−$N_{oxamidate}$ and 2.093(2) Å for the Mo−$O_{oxamidate}$ bonds.[17] This MV species is electronically delocalized, and it is appropriate to formally assign a half valence to each of the Mo_2 centers, $[Mo_2]^{0.5+}$(di-*p*-anisyloxamidate)$[Mo_2]^{0.5+}$.

The two doubly oxidized compounds **3** and **4** constitute the third α/β isomer pair in this system. The core structures of the dications in each compound are shown in Figure 1. For **3** (α^{2+}), the two Mo−Mo bond lengths are essentially the same, 2.1248(9) and 2.1243(11) Å, and chemically indistinguishable from that in the oxidized site of its precursor **1** (2.1291(6) Å). In **3**, each of the dimolybdenum units has an Mo_2^{5+} core with a bond order of 3.5 derived from the electronic configuration $\sigma^2\pi^4\delta^1$. Similarly, the β isomer (**4**) also has two lengthened Mo−Mo bonds, which are 2.1449(8) and 2.1418(8) Å. It is interesting to note that the metal−metal bonds in **4** are slightly longer than those in **3**, even though the formal oxidation states are the same. The increase in Mo−Mo bond distances is 0.037 Å for the α isomer but 0.049 Å for the β, as two electrons are removed. We have been unable to find a straightforward explanation for such difference. However, it appears that the difference is not due to the α/β binding mode because in the two neutral

(19) Cotton, F. A.; Liu, C. Y.; Murillo, C. A.; Villagrán, D.; Wang, X. *J. Am. Chem. Soc.* **2004**, *126*, 14822.

Table 1. Selected Bond Lengths (Å) and Angles (deg)

compound	**1**·4CH_2Cl_2	**2**·3.5CH_2Cl_2	**3**·3CH_2Cl_2	**4**·2CH_2Cl_2
Mo(1)−Mo(2)	2.0920(6)	2.1116(7)	2.1236(8)	2.1449(8)
Mo(3)−Mo(4)	2.1291(6)	2.1140(6)	2.1254(8)	2.1416(8)
Mo_2···Mo_2[a]	7.051	6.273	7.070	6.211
Mo(1)−N(1)	2.197(4)	2.147(4)	2.164(4)	2.109(4)
Mo(2)−O(1)	2.121(3)	2.054(3)	2.134(4)	2.026(4)
Mo(3)−N(2)	2.166(4)	2.141(4)	2.175(4)	2.118(5)
Mo(4)−O(2)	2.105(3)	2.058(3)	2.122(4)	2.016(4)
Mo(1)−N(3)	2.166(4)	2.179(4)	2.138(5)	2.167(4)
Mo(1)−N(5)	2.153(4)	2.167(4)	2.130(5)	2.104(5)
Mo(1)−N(7)	2.161(4)	2.154(4)	2.162(5)	2.160(4)
Mo(2)−N(4)	2.129(4)	2.133(4)	2.102(5)	2.119(4)
Mo(2)−N(6)	2.129(4)	2.103(4)	2.117(5)	2.107(5)
Mo(2)−N(8)	2.136(4)	2.106(4)	2.093(5)	2.063(4)
Mo(3)−N(9)	2.121(4)	2.176(4)	2.152(5)	2.140(5)
Mo(3)−N(11)	2.112(4)	2.174(4)	2.131(5)	2.162(4)
Mo(3)−N(13)	2.145(4)	2.136(4)	2.123(5)	2.120(5)
Mo(4)−N(10)	2.123(4)	2.110(4)	2.114(5)	2.114(5)
Mo(4)−N(12)	2.089(4)	2.129(4)	2.093(5)	2.096(5)
Mo(4)−N(14)	2.120(4)	2.111(4)	2.111(5)	2.106(5)
N(1)−C(1)	1.305(6)		1.317(7)	
N(2)−C(2)	1.308(6)		1.302(7)	
N(1)−C(2)		1.324(6)		1.310(7)
N(2)−C(1)		1.323(6)		1.319(7)
O(1)−C(1)	1.282(6)	1.287(5)	1.265(6)	1.283(6)
O(2)−C(2)	1.290(5)	1.277(5)	1.274(6)	1.291(6)
C(1)−C(2)	1.528(6)	1.507(6)	1.533(7)	1.516(7)
Mo(1)−Mo(2)−O(1)	95.09(9)	99.38(8)	93.57(10)	98.82(10)
Mo(2)−Mo(1)−N(1)	89.63(10)	98.84(10)	90.25(12)	99.43(12)
Mo(3)−Mo(4)−O(2)	94.04(8)	98.90(9)	93.78(10)	100.11(10)
Mo(4)−Mo(3)−N(2)	89.58(10)	99.92(9)	89.59(12)	98.34(12)

[a] Distance between the midpoints of the two dimolybdenum units.

precursors, the metal−metal bond distances are essentially the same.[17] Along with the difference in metal−metal bond distances, the metal−ligand distances in **4** are shorter, on average, than those in **3** (Table 1), implying that the Mo_2 units in **4** are more positively charged than those in **3**. In general, the effect of lowering electron density on the dimetal core should increase the metal−metal bond distance. This is understandable if the metal-to-ligand back-π-bonding in **4**, the delocalized compound, is greater than that for **3**.

Near-IR Spectroscopy. Different spectroscopic properties for the two isomers were first observed in CH_2Cl_2 solutions of the MV species generated in situ by mixing each of the corresponding neutral precursors with 1 equiv of oxidizing reagent $(Cp_2Fe)PF_6$.[17] We now report results obtained using crystalline samples of **1** and **2** in KBr pellets. The spectra, recorded in the range of 2000−8000 cm^{-1}, are shown in Figure 2. The β isomer, **2**, exhibits an intense absorption band centered at ca. 4730 cm^{-1}, while the spectrum of the α isomer is devoid of absorption bands in the NIR region. This spectrum of **2** measured in a solid sample is very similar to that obtained in CH_2Cl_2 solution, in which the transition was measured at 4700 cm^{-1}.[17] The bandwidth at half-height, $\Delta\nu_{1/2}$, of 2300 cm^{-1} is significantly smaller than the value of 3300 cm^{-1} calculated for a charge-transfer transition of a class II species using the Hush formula, $\Delta\nu_{1/2} = (2310\ \Delta\nu_{max})^{1/2}$.[20] A narrower band suggests that the electronic coupling interaction is stronger than that for a class II species, which is consistent with the structural data. The strong band in the NIR spectrum of this delocalized species may be described as a HOMO−1 → SOMO transition.

(20) Hush, N. S. *Coord. Chem. Rev.* **1985**, *64*, 135.

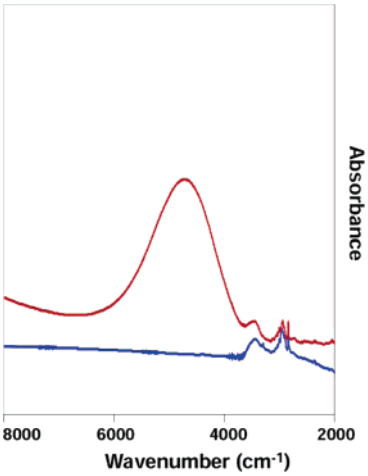

Figure 2. Near-IR spectra of the crystalline mixed-valence species **1** (in blue) and **2** (in red) in KBr pellets.

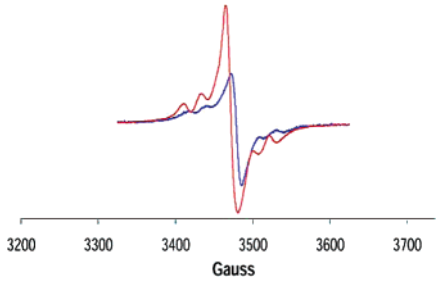

Figure 3. EPR spectra of **1** (in blue) and **3** (in red) in CH_2Cl_2 solution at ambient temperature.

Additional support for the latter idea comes from a study employing DFT calculations which showed that in the β form,[17] the frontier MOs are derived from the combination of the metal δ orbitals with significant involvement of the ligand π orbitals. For the singly oxidized species **2**, the odd electron resides in a delocalized molecular orbital (SOMO), having electron density equally distributed over the two $[Mo_2]$ units. For the analogous complex β-{$[Mo_2]$(dimethyloxamidate)$[Mo_2]$}$^+$, it was found that an electronic transition (HOMO−1 → SOMO) at relatively low energy corresponds to the absorption band in the near-IR spectrum.[19] For the α compound (**1**), however, the situation is quite different. DFT calculations on the neutral α precursor[17] have shown that the molecule has two localized $[Mo_2]$ units that do not interact significantly with each other and thus no intervalence charge-transfer band is observed.

EPR Spectra. X-band electron paramagnetic resonance (EPR) spectroscopy has also been employed for the study of **1**−**4**, all of which have formally one or two Mo_2^{5+} units. For the two paramagnetic compounds in α form (**1** and **3**), the EPR spectra were measured at room temperature in CH_2Cl_2 solution. For each compound, the spectrum shows one prominent symmetric peak having some hyperfine structure (Figure 3). The spectra for these two species are similar, with little difference in the *g* value. Importantly, the *g* values, 1.950 for **1** and 1.951 for **3**, are significantly smaller than the value expected for a free organic radical, indicating that odd electron resides in a metal-based orbital. For **3**, this result provides further evidence that there are two linked but

Table 2. EPR Simulation Parameters

compound	**1**	**2**	**3**	**4**
g value	1.950	1.947	1.951	
A ($\times 10^{-4}$ cm^{-1})	21	11	21	diamagnetic

essentially uncoupled Mo_2^{5+} units forming a diradical. The main signal is attributed to molecules containing only the ^{96}Mo ($I = 0$) isotope, while the hyperfine structure is due to molecules with one ^{95,97}Mo ($I = 5/2$) isotope, which has a natural abundance of about 25%.[21] For both **1** and **3** spectral simulations were done using a localized model with one odd electron residing on an Mo_2 unit. As shown in Table 2, by using the parameters $g = 1.950$ and $A = 21 \times 10^{-4}$ cm^{-1}, similar to those in the parent paddlewheel cation $[Mo_2(DAniF)_4]^+$,[22] the simulated spectra show satisfactory agreement with the experimental results.

The spectrum for the singly oxidized species **2** in the β form, measured in solution at -60 °C,[23] exhibits a prominent peak ($g = 1.947$) and several hyperfine lines (Figure 4). However, simulation gives a hyperfine coupling constant $A = 11 \times 10^{-4}$ cm^{-1}, which is about half of that for **1** (Table 2). Prior studies on various MV species of the type $\{[Mo_2]L[Mo_2]\}^+$ have shown that electronic delocalization over two Mo_2 units has the effect of lowering the constant A. For example, for the delocalized complex $\{[Mo_2](\text{dioxolenate})[Mo_2]\}^+$,[16] the hyperfine coupling constant A was 12.2×10^{-4} cm^{-1}, while for the weakly coupled compound $\{[Mo_2](N,N'\text{-diethylterephthalamidate})[Mo_2]\}^+$, the A value is 22×10^{-4} cm^{-1}.[24] Chisholm and co-workers have reported that the dimolybdenum pairs linked by oxalate and perfluoroterephthalate, which differ largely in the extent of electronic delocalization, have hyperfine coupling constants of 14.8 and 27.2 G (14.8×10^{-4} and 27.2×10^{-4} cm^{-1}, respectively.)[11f]

Unlike **1**−**3**, which are paramagnetic, complex **4** is diamagnetic, as shown by the observation of both sharp signals of the ^{1}H NMR spectrum and because it is EPR silent.[25] Diamagnetism for complexes that have two linked, magnetically equivalent metal complex subunits could result from either metal−metal antiferromagnetic exchange interaction or from pairing of spins by electrons occupying the same delocalized MO. In our previous studies on dimolybdenum pairs, diamagnetic behaviors have been observed for several complexes with different linkers, for example, β-$\{[Mo_2](\text{dimethyloxamidate})[Mo_2]\}^{2+}$,[19] $\{[Mo_2](\text{fluoflavinate})[Mo_2]\}^{2+}$,[15] and $\{[Mo_2](\mu\text{−OR})_4[Mo_2]\}^{2+}$.[26] In all of these compounds the outer electrons are paired up in the same MO.

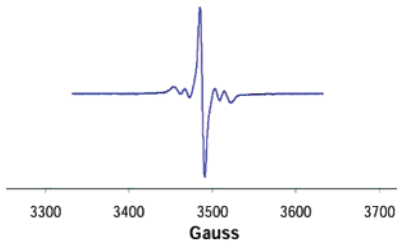

Figure 4. EPR spectrum of **2** at −60 °C in CH_2Cl_2 solution.

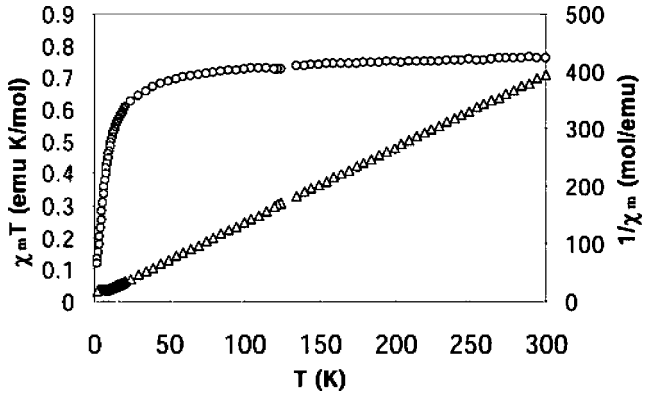

Figure 5. Plots of $\chi_m T$ (○) and $1/\chi_m$ (△) vs temperature for **3**.

Magnetic Measurements. Because formally each of the doubly oxidized compounds **3** and **4** has one unpaired electron at each of the two $[Mo_2]$ units, they offer an excellent opportunity for the study the magnetic behavior of a system with two spatially separated odd electrons. For such compounds, the possible interaction patterns include (1) no coupling, (2) ferromagnetic coupling, and (3) antiferromagnetic coupling. The first case is simply the combination of its parts; it possesses only local spins, each with $S = 1/2$. Ferromagnetic coupling would generate a triplet ground state, $S = 1$, and antiferromagnetic coupling would yield a singlet ground state, $S_T = 0$. Calculated values of $\chi_m T$ (emu K mol^{-1}) in the limit $T \rightarrow 0$ K, using in each case a spin-only model with $g = 2.00$, are 0.75, 1, and 0 for each of the three cases, respectively. A variable-temperature study of the bulk magnetic susceptibility of **3**, Figure 5, shows a value of $\chi_m T$ of 0.76 emu K mol^{-1} that is essentially independent of T in the range of 50−300 K, while magnetic measurements of **4** give a $\chi_m T$ value close to 0 emu K mol^{-1}.[27] This is conclusive evidence that there is no significant spin coupling, either ferromagnetic or antiferromagnetic, in **3** (α^{2+}) and that the two unpaired electrons in **4** (β^{2+}) are antiferromagnetically coupled.

Conclusions

In an earlier report we had shown that two linkage isomers containing dimolybdenum units with bridged oxamidate dianions have large differences in electronic communication with K_c values being about 10^6 times larger for

(21) For an early example of the use of Mo isotopes for establishing mixed valence, see Bruns, W.; Kaim, W.; Waldör, E.; Krejčik, M. *J. Chem. Soc., Chem. Commun.* **1993**, 1868.
(22) Cotton, F. A.; Donahue, J. P.; Huang, P.; Murillo, C. A.; Villagrán, D.; Wang, X. *Z. Anorg. Allg. Chem.* **2005**, *631*, 2606.
(23) The EPR spectrum of **2** at room temperature gives the same *g* value and hyperfine structure.
(24) Cotton, F. A.; Li, Z.; Liu, C. Y.; Murillo, C. A. *Inorg. Chem.* **2006**, *45*, 9765.
(25) To obtain a clean ^{1}H NMR spectrum of **4** (β^{2+}) with sharp signals, it is important to add a small amount of iodine to oxidize a trace of **2** (β^+) present as an impurity in solution. The EPR spectra of **4** (β^{2+}) also showed a small amount of **2** (β^+). Its EPR signal also disappeared upon addition of a small amount of iodine. These observations are consistent with **4** (β^{2+}) being diamagnetic.
(26) Cotton, F. A.; Li, Z.; Liu, C. Y.; Murillo, C. A.; Zhao, Q. *Inorg. Chem.* **2006**, *45*, 6387.
(27) This value is typically less than 0.10 emu K mol^{-1} and independent of *T*. Such background value is due to the existence of a small amount of contamination from the singly oxidized β^+ species. See ref 25.

the β form which has two six-membered rings formed by the Mo−Mo−N−C−C−O groups than for the α form.[17] Unfortunately, the neutral compounds (especially that in the β form) had been obtained in low yields and isolation of the pure products was difficult. This hampered further study of this interesting system. Here, we report syntheses that give higher yields of the α and β products with good purity, as well as the structures, NIR, and EPR spectra of the α^+, α^{2+}, β^+, and β^{2+} species. The results unambiguously show that the α^+ species is electronically localized while the β^+ species is delocalized. We also confirm that while the α^{2+} species is a diradical, the β^{2+} species is essentially diamagnetic. Using these isomers, we demonstrate how important the conformation of the linker is in mediating electronic communication between metal-containing units.

Experimental Section

Materials and Methods. Solvents were dried and then distilled under N_2 following conventional methods or purified under argon using a Glass Contour solvent purification system. The syntheses of **1**−**4** were conducted under N_2 using Schlenk line techniques. $Mo_2(DAniF)_3(O_2CCH_3)$,[17,28] *N*,*N*′-di-*p*-anisyloxamide,[17] and HDAniF[29] were prepared by following published methods; 0.5 M solution of $NaOCH_3$ in methanol, purchased from Aldrich, was used as received. Ferrocenium hexafluorophosphate, $(Cp_2Fe)PF_6$, was purified by recrystallization from acetone/hexane prior to use.

Physical Measurements. Elemental analyses were performed by Robertson Microlit Laboratories, Madison, NJ. ^{1}H NMR spectra were recorded at 25 °C on a Mercury-300 NMR spectrometer with chemical shifts (δ, ppm) referenced to $CDCl_3$. Electronic spectra in the UV−vis range were measured in the range of 200−800 nm on a Shimadzu UV-2501PC spectrophotometer. The NIR spectra were obtained from a Bruker TEASOR 27 spectrometer. EPR spectra were recorded using a Bruker ESP300 spectrometer, and the simulations of the spectra were performed using the program WIN-EPR SimFonia from Bruker. Measurement of magnetic susceptibility was performed on a SQUID magnetometer.

Improved Preparation of α-[Mo_2(DAniF)$_3$]$_2$(*N*,*N*′-di-*p*-anisyloxamidate). $Mo_2(DAniF)_3(O_2CCH_3)$ (0.51 g, 0.50 mmol) and *N*,*N*′-di-*p*-anisyloxamide (0.075 g, 0.25 mmol) were mixed in 20 mL of tetrahydrofuran. To the mixture, with stirring, was added 1.0 mL of a $NaOCH_3$ solution (0.50 M in CH_3OH), giving an orange solution. After stirring at ambient condition for 48 h, a yellow solid formed. The solvent was removed by evaporation under vacuum. The residue was extracted by dichloromethane, then filtered through a Celite-packed frit. The volume of the filtrate was reduced to about 5 mL. A yellow solid was produced by addition of hexanes (ca. 30 mL) to the concentrated solution. Finally, the solid product was collected by filtration and dried under vacuum. Yield: 0.46 g (82%). This material was used for the oxidation reactions without further purification.

Improved Preparation of β-[Mo_2(DAniF)$_3$]$_2$(*N*,*N*′-di-*p*-anisyloxamidate). $Mo_2(DAniF)_3(O_2CCH_3)$ (0.51 g, 0.50 mmol) and *N*,*N*′-di-*p*-anisyloxamide (0.075 g, 0.25 mmol) were mixed in 20 mL of tetrahydrofuran. To the mixture, with stirring, was added 1.0 mL of a $NaOCH_3$ solution (0.5 M in CH_3OH), giving an orange solution. The solution was stirred for 30 min, and then, the solvent was removed by evaporation under vacuum. The residue was extracted with dichloromethane (ca. 20 mL) and filtered through a Celite-packed frit. With stirring, the filtrate was transferred, through a cannula, to hot enthanol, generating a red precipitate. The mixture was stirred at ∼80 °C for 30 min, then filtered while it was hot. The red solid was washed with 10 mL of hot ethanol and finally dried under vacuum. Yield: 0.23 g (41%). This material was used for the oxidation reaction without further purification.

Preparation of α-[Mo_2(DAniF)$_3$]$_2$(*N*,*N*′-di-*p*-anisyloxamidate)-PF_6, 1. A yellow solution of α-[Mo_2(DAniF)$_3$]$_2$(*N*,*N*′-di-*p*-anisyloxamidate) (0.140 g, 0.063 mmol) in 10 mL of CH_2Cl_2 and a blue solution having 1 equiv of $(Cp_2Fe)PF_6$ in 10 mL of CH_2Cl_2 were prepared separately and cooled to −78 °C. The two solutions were mixed by transferring the oxidizing reagent to the dimolybdenum complex using a cannula. After the resultant solution was stirred at −78 °C for 30 min, 60 mL of precooled hexanes was added by syringe to produce a dark brown precipitate. After the solvent was decanted, the solid residue was washed with 20 mL of hexanes and then dried under vacuum. The solid was dissolved in dichloromethane, and the solution was then layered with hexanes. Large dark crystals were obtained after diffusion for a period of 3 days. Yield: 0.081 g (54%). UV−vis in CH_2Cl_2, λ_{max} (nm) (ϵ, M^{-1} cm^{-1}): 442 (3.3×10^3). Anal. Calcd for $C_{106}H_{104}F_6Mo_4N_{14}O_{16}P$ (**1**): C, 53.97; H, 4.44; N, 8.31. Found: C, 54.09; H, 4.18; N, 8.21.

Preparation of β-[Mo_2(DAniF)$_3$]$_2$(*N*,*N*′-di-*p*-anisyloxamidate)-PF_6, 2. This black compound was synthesized using a procedure similar to that for **1**, where red β-[Mo_2(DAniF)$_3$]$_2$(*N*,*N*′-di-*p*-anisyloxamidate) and 1 equiv of Cp_2FePF_6 were used as the starting materials. Large block-shaped crystals of **2**·3.5CH_2Cl_2 were obtained. Yield: 0.071 g (89%). NIR (KBr, cm^{-1}): 4730 (vs). UV−vis in CH_2Cl_2, λ_{max} (nm) (ϵ, M^{-1} cm^{-1}): 433 (3.4×10^3), 566 (1.3×10^3), 630 (7.2×10^3). Anal. Calcd for $C_{107}H_{106}Cl_2F_6Mo_4N_{14}O_{16}P$ (**2**·CH_2Cl_2): C, 52.59; H, 4.37; N, 8.02. Found: C, 52.38; H, 3.97; N, 7.94.

Preparation of α-[Mo_2(DAniF)$_3$]$_2$(*N*,*N*′-di-*p*-anisyloxamidate)-(PF_6)$_2$, 3. This compound was prepared similarly to **1** using α-[Mo_2(DAniF)$_3$]$_2$(*N*,*N*′-di-*p*-anisyloxamidate) (0.12 g, 0.055 mmol) and 2 equiv of $(Cp_2Fe)PF_6$ (0.036 g, 0.11 mmol) in 15 mL of CH_2Cl_2. Small black crystals were obtained. Yield: 0.077 g (56%). UV−vis in CH_2Cl_2, λ_{max} (nm) (ϵ, M^{-1} cm^{-1}): 450 (8.7×10^4). Anal. Calcd for $C_{106}H_{104}F_{12}Mo_4N_{14}O_{16}P_2$ (**3**): C, 50.85; H, 4.19; N, 7.83. Found: C, 50.50; H, 3.74; N, 7.70.

Preparation of β-[Mo_2(DAniF)$_3$]$_2$(*N*,*N*′-di-*p*-anisyloxamidate)-(PF_6)$_2$, 4. This black compound was synthesized using a procedure similar to that for **2**, using 2 equiv of oxidizing regent. Small block-shaped crystals of **4**·2CH_2Cl_2 were obtained. Yield: 0.069 g (82%). ^{1}H NMR at 25 °C (in $CDCl_3$): 6.62 (d, 4H, aromatic C−*H*), 6.41 (m, 24H, aromatic C−*H*), 6.11 (m, 24H, aromatic C−*H*), 5.85 (d, 4H, aromatic C−*H*), 3.77 (s, 6H, −OC*H*$_3$), 3.65 (s, 12H, −OC*H*$_3$), 3.56 (s, 12H, −OC*H*$_3$), 3.50 (s, 6H, −OC*H*$_3$), 3.47 (s, 6H, −OC*H*$_3$). ^{1}H NMR at −50 °C (in $CDCl_3$): 8.93 (s, 6H, −NC*H*N−), 6.57 (d, 4H, aromatic C−*H*), 6.42 (m, 24H, aromatic C−*H*), 6.05 (m, 24H, aromatic C−*H*), 5.86 (d, 4H, aromatic C−*H*), 3.77 (s, 6H, −OC*H*$_3$), 3.66 (s, 12H, −OC*H*$_3$), 3.54 (s, 12H, −OC*H*$_3$), 3.48 (s, 6H, −OC*H*$_3$), 3.45 (s, 6H, −OC*H*$_3$). UV−vis in CH_2Cl_2, λ_{max} (nm) (ϵ, M^{-1} cm^{-1}): 464 (1.0×10^4), 598 (787), 731 (1.3×10^4), 876 (7.2×10^3). Anal. Calcd for $C_{107}H_{106}Cl_2F_{12}Mo_4N_{14}O_{16}P_2$ (**4**·CH_2Cl_2): C, 49.65; H, 4.13; N, 7.58. Found: C, 49.25; H, 4.35; N, 7.13.

X-ray Structure Determinations. Single crystals suitable for X-ray analysis were mounted and centered on the tips of cryoloops. Then each crystal was attached to a goniometer head. Data for **1**·4CH_2Cl_2, **2**·3.5CH_2Cl_2, **3**·3CH_2Cl_2, and **4**·2CH_2Cl_2 were collected at −60 °C on a BRUKER SMART 1000 CCD area detector system.

(28) Stephenson, T. A.; Bannister, E.; Wilkinson, G. *J. Chem. Soc.* **1964**, 2538.
(29) Lin, C.; Protasiewicz, J. D.; Ren, T. *Inorg. Chem.* **1996**, *35*, 6422.

Table 3. X-ray Crystallographic Data

compound	**1**·4CH_2Cl_2	**2**·3.5CH_2Cl_2	**3**·3CH_2Cl_2	**4**·2CH_2Cl_2
empirical formula	$C_{110}H_{112}Cl_8F_6Mo_4N_{14}O_{16}P$	$C_{109.5}H_{111}Cl_7F_6Mo_4N_{14}O_{16}P$	$C_{109}H_{110}Cl_6F_{12}Mo_4N_{14}O_{16}P_2$	$C_{108}H_{108}Cl_4F_{12}Mo_4N_{14}O_{16}P_2$
fw	2698.47	2656.00	2758.51	2673.58
space group	$P2_1/c$ (No.14)	$P\bar{1}$ (No. 2)	$P\bar{1}$ (No. 2)	$P\bar{1}$ (No. 2)
a (Å)	14.2863(7)	16.186(3)	15.905(4)	16.489(5)
b (Å)	15.7924(8)	18.231(3)	19.349(5)	17.873(5)
c (Å)	52.946(3)	21.990(4)	21.638(5)	20.498(6)
α (deg)	90	93.145(3)	72.397(5)	74.728(5)
β (deg)	93.432(2)	110.568(3)	79.210(5)	75.070(5)
γ (deg)	90	108.078(3)	69.398(4)	80.877(6)
V (Å^3)	11924(1)	5677(2)	5917(2)	5604(3)
Z	4	2	2	2
T (K)	213	213	213	213
d_{calcd} (g/cm^3)	1.503	1.554	1.548	1.584
μ (mm^{-1})	0.680	0.690	0.663	0.651
R1[a] (wR2[b])	0.077 (0.133)	0.064 (0.138)	0.086 (0.166)	0.090 (0.165)

[a] $R1 = \sum||F_o| - |F_c||/\sum|F_o|$. [b] $wR2 = [\sum[w(F_o^2 - F_c^2)^2]/\sum[w(F_o^2)^2]]^{1/2}$.

Cell parameters were determined using the program SMART.[30] Data reduction and integration were performed with the software package SAINT,[31] while absorption corrections were applied using the program SADABS.[32] The positions of the heavy atoms were found via direct methods using the program SHELXTL.[33] Subsequent cycles of least-squares refinement followed by difference Fourier syntheses revealed the positions of the remaining non-hydrogen atoms. Hydrogen atoms were added in idealized positions. Non-hydrogen atoms, except some atoms from disordered methoxyl groups and solvent molecules, were refined with anisotropic displacement parameters. Crystallographic data for **1**·4CH_2Cl_2, **2**·3.5CH_2Cl_2, **3**·3CH_2Cl_2, and **4**·2CH_2Cl_2 are given in Table 3, and selected bond distances and angles in Table 1.

Acknowledgment. We thank the Robert A. Welch Foundation and Texas A&M University for financial support. We also thank Mark Young, Penglin Huang, Sergey Ibragimov, and Dino Villagrán for their help with the magnetic and EPR measurements.

Supporting Information Available: X-ray crystallographic data for **1**·4CH_2Cl_2, **2**·3.5CH_2Cl_2, **3**·3CH_2Cl_2, and **4**·2CH_2Cl_2 in standard CIF format. This material is available free of charge via the Internet at http://pubs.acs.org.

IC0622252

(30) *SMART V 5.05 Software for the CCD Detector System*; Bruker Analytical X-ray System, Inc.: Madison, WI, 1998.
(31) *SAINT Data Reduction Software. V 6.36A*; Bruker Analytical X-ray System, Inc.: Madison, WI, 2002.
(32) *SADABS. Bruker/Siemens Area Detector Absorption and Other Corrections. V2.03*; Bruker Analytical X-ray System, Inc.: Madison, WI, 2002.
(33) Sheldrick, G. M. *SHELXTL. V 6.12*; Bruker Analytical X-ray Systems, Inc.: Madison, WI, 2000.